Original Article

MOLECULAR METABOLISM

β-catenin regulates muscle glucose transport via actin remodelling and M-cadherin binding

Stewart W.C. Masson [1,2], Brie Sorrenson [3], Peter R. Shepherd [2,3], Troy L. Merry [1,2,*]

ABSTRACT

Objective: Skeletal muscle glucose disposal following a meal is mediated through insulin-stimulated movement of the GLUT4-containing vesicles to the cell surface. The highly conserved scaffold-protein β-catenin is an emerging regulator of vesicle trafficking in other tissues. Here, we investigated the involvement of β-catenin in skeletal muscle insulin-stimulated glucose transport.

Methods: Glucose homeostasis and transport was investigated in inducible muscle specific β-catenin knockout (BCAT-mKO) mice. The effect of β-catenin deletion and mutation of β-catenin serine 552 on signal transduction, glucose uptake and protein—protein interactions were determined in L6-G4-myc cells, and β-catenin insulin-responsive binding partners were identified via immunoprecipitation coupled to label-free proteomics.

Results: Skeletal muscle specific deletion of β-catenin impaired whole-body insulin sensitivity and insulin-stimulated glucose uptake into muscle independent of canonical Wnt signalling. In response to insulin, β-catenin was phosphorylated at serine 552 in an Akt-dependent manner, and in L6-G4-myc cells, mutation of β-catenin^{S552} impaired insulin-induced actin-polymerisation, resulting in attenuated insulin-induced glucose transport and GLUT4 translocation. β-catenin was found to interact with M-cadherin in an insulin-dependent β-catenin^{S552}-phosphorylation dependent manner, and loss of M-cadherin in L6-G4-myc cells attenuated insulin-induced actin-polymerisation and glucose transport.

Conclusions: Our data suggest that β-catenin is a novel mediator of glucose transport in skeletal muscle and may contribute to insulin-induced actin-cytoskeleton remodelling to support GLUT4 translocation.

Keywords Beta-catenin; Actin-remodelling; Glucose transport; M-cadherin; GLUT4 trafficking

1. INTRODUCTION

Skeletal muscle is the largest site of insulin-stimulated glucose disposal following a meal, and skeletal muscle glucose utilisation is impaired in insulin resistance and type 2 diabetes [1]. The transport of glucose into muscle is predominantly mediated by the movement of glucose transporter 4 (GLUT4) to the cell membrane in response to insulin, which is regulated by at least two divergent signalling cascades that share similar upstream regulators. The best characterised of these pathways involves PI3k/Akt mediated phosphorylation of Akt-substrate of 160 kD (AS160/TBC1D4) [2,3], which results in the inhibition of GTPase activity, triggering translocation and fusion of GLUT4-containing vesicles (GCVs). The second involves remodelling of the actin cytoskeleton at the cell membrane, thereby providing the physical structure to facilitate the movement of GCV within the cell [4—9]. While localised actin remodelling is critical for optimal insulin-stimulated glucose uptake in skeletal muscle [6], many putative insulin-induced actin regulators, such as PAK1 [10] appear to be somewhat dispensable suggesting that there are alternative regulators of insulin-dependent GLUT4 trafficking.

Beta-catenin is a highly conserved structural protein that links the actin cytoskeleton to cell—cell cadherin junctions via its ubiquitous binding partner α-catenin [11—13]. Canonically, β-catenin is best recognised as the downstream effector of Wnt signalling, in which levels of β-catenin are regulated by a Wnt ligand-inhibited degradation complex, leading to accumulation of the protein and activation of Wnt target genes [14,15]. However, it has been identified in cross-species screens as a candidate gene involved in the development of insulin-resistance [16] and also implicated in the regulation of GLUT4 trafficking in adipocytes [17]. Many of the proteins involved in insulin signalling, including Akt, PAK1 and Rac1, are known to modulate β-catenin function in non-muscle cells, as well as insulin-induced actin remodelling [4,18—20]. This indicates a need to understand the mechanisms by which β-catenin is involved in regulating glucose transport and actin remodelling.

Here, we investigated whether β-catenin is required for insulin-mediated glucose transport in skeletal muscle. We report that depletion of β-catenin impairs insulin-stimulated skeletal muscle glucose transport and induces whole body insulin resistance. We also provide evidence that insulin-induced phosphorylation of β-catenin^{S552} is

[1]Discipline of Nutrition, Faculty of Medical and Health Sciences, The University of Auckland, Auckland, New Zealand [2]Maurice Wilkins Centre for Molecular Biodiscovery, The University of Auckland, Auckland, New Zealand [3]Department of Molecular Medicine and Pathology, Faculty of Medical and Health Sciences, The University of Auckland, Auckland, New Zealand

*Corresponding author. 85 Park Road, Grafton, Auckland, New Zealand. E-mail: t.merry@auckland.ac.nz (T.L. Merry).

Received August 13, 2020 • Revision received September 17, 2020 • Accepted September 24, 2020 • Available online 1 October 2020

https://doi.org/10.1016/j.molmet.2020.101091

mediated by proximal insulin signalling and facilitates β-catenin binding with M-cadherin to control insulin-mediated actin cytoskeleton remodelling and that these events play an important role in regulating GLUT4 trafficking.

2. MATERIALS AND METHODS

2.1. Antibodies and reagents

All reagents, unless otherwise stated, were purchased from Sigma—Aldrich Chemicals (St. Louis, MO, USA). Antibodies and primer sequences are listed in Supplementary Tables 1 and 2, respectively.

2.2. Murine breeding and housing conditions

Mice were maintained in groups of 4—10 per cage at 20 °C in a temperature-controlled animal facility with a 12-h light—dark cycle and *ad libitum* access to water and a standard rodent chow diet (Teklad TB 2018; Harlan, Madison, WI, USA). All experiments were approved by the University of Auckland animal ethics committee, Auckland, New Zealand. Inducible muscle-specific β-catenin-deficient mice were generated by crossing β-catenin^{flox} (B6.129-Ctnnb1^{tm2Kem}/KnwJ) and HSA-MCM Cre (Tg(ACTA1-cre/Esr1*)2Kesr/J) mice (obtained from Jackson Laboratories, USA, stock numbers #0044152 and #025750), resulting in β-catenin$^{lox/+;CreMCM-/+}$, which are referred to as BCAT-mKO, where m stands for muscle [21,22]. β-catenin$^{lox/+;CreMCM-/-}$ littermates were used as control (wild-type, WT) mice. Cre expression was induced at 8—12 weeks of age by administration of 2 mg of tamoxifen (Cayman Chemicals, Michigan, USA) via oral gavage for 5 consecutive days. WT and BCAT-mKO mice received the same dose of tamoxifen. Only male mice were used for experiments due to the inability to induce significant β-catenin knockdown in female mice.

2.3. Mouse metabolic measures

For metabolic cage experiments, mice were single housed at 23 °C. Food and water intake, ambulatory activity, energy expenditure and respiratory exchange ratio was determined using a Promethion High-Definition Multiplexed Respirometry System (Sable Systems International, Las Vegas, NV, USA). Fed and fasted (overnight) blood samples were collected via submandibular bleeding, and blood glucose was determined using a hand-held glucose meter (Accu-Chek Performa; Roche, Basal, Switzerland). Plasma insulin was determined using an AlphaLISA immunoassay detection kit (PerkinElmer, Waltham, MA). For insulin tolerance tests, mice were fasted for 4 h (1000—1400 h), and blood glucose measurements were taken at the time points indicated after an intraperitoneal injection of 0.7 mU/g of Actrapid insulin (Novo Nordisk, Bagsværd, Denmark). For glucose tolerance tests, mice were fasted overnight prior to oral gavage with 1 mg/g of glucose, and blood glucose measures were taken as indicated. Running performance was determined using a Touchscreen treadmill, model 76-0896 (Panlab/Harvard Apparatus, Holliston, MA, USA). Mice began at 5 cm/s without incline, which increased steadily at 2.5 cm/s/min. All mice ran to failure, defined as resting on the shock grid (0.3 mA shock stimulus) for more than 5 s. For the determination of *in vivo* signalling C57BL/6j mice were fasted for 4 h prior to intraperitoneal injections of either saline or insulin (5 mU/g) or oral gavages of glucose (2 mg/kg). Mice were culled by cervical dislocation at either 10 min (insulin) or 30 min (insulin and glucose) post-treatment and tissues were rapidly dissected. All tissues were snap frozen in liquid nitrogen for further analysis.

2.4. *In vivo* glucose uptake

In vivo glucose uptake was determined essentially as previously described [23]. Twenty-week-old BCAT-mKO and WT mice were fasted for 4 h (1000—1400 h) prior to intraperitoneal injection with radiolabelled 2-[2,6-3H]-2 deoxy-D-glucose, specific activity 0.128 μCi ml-1, (100 μl of phosphate-buffered saline (PBS)/animal, 1 mCi/ml) and either 1 mU/g of insulin or a PBS control. After 30 min, mice were culled, and tissues were quickly washed in ice-cold PBS and snap frozen in liquid nitrogen. Quantification of uptake was determined as previously described [24]. A portion of tissue was lysed in 1 M of NaOH, followed by neutralisation in 1 M of HCl. Lysate was then deproteinised in perchloric acid (to yield total 2-DG) and equal volumes of BaOH and $ZnSO_4$ (to yield unphosphorylated 2-DG). The difference (phosphorylated 2-DG) was then expressed relative to brain phosphorylated 2-DG.

2.5. *Ex vivo* glucose uptake

Ten week-old male BCAT-mKO and WT mice were anaesthetised with intraperitoneal injection of pentobarbitone. Then, the extensor digitorum longus (EDL) and soleus muscles were excised and brought to optimal length in Krebs-Heinsleit buffer (KHB; 118.5 mM NaCl, 24.7 mM $NaHCO_3$, 4.74 mM KCl, 1.18 mM $MgSO_4$, 1.18 mM KH_2PO_4, 2.5 mM $CaCl_2$, 8 mM mannitol, 2 mM pyruvate, 0.01% bovine serum albumin (BSA), pH 7.4), bubbled with carbogen (95% O_2, 5% CO_2) and maintained at 25 °C. Muscles were then stimulated with insulin (100 nM) for 20 min prior to incubation in modified KHB containing radiolabelled 2-DG and mannitol (KHB; 8 mM mannitol, 1 mM 2DG, 2-[2,6-3H]-2DG, and [1-14C] mannitol, specific activity 0.083 μCi ml-1). Muscle was washed in ice cold PBS and immediately snap-frozen in liquid nitrogen before being weighed and homogenised in 1 M of NaOH and radioactivity read in a Perkin Elmer Quantulus GCT Liquid Scintillation Counter (Perkin Elmer, Waltham, MA, USA), and glucose transport was calculated as described previously [25].

2.6. Cell culture

L6-G4-myc myoblasts (Kerafast, Boston, MA, USA) were grown in low-glucose Dulbecco's modified Eagle's medium (DMEM) supplemented with 10% foetal bovine serum and 1% penicillin/streptomycin. Differentiation was induced by changing media to low-glucose DMEM supplemented with 2% horse serum for 2—3 days. Akt inhibitor AKTi-1/2 (10 μM), the p110α isoform of PI3k inhibitor, BYL719 (5 μM) or the Rac1 inhibitor NSC23766 (200 μM) were added to cells 1 h prior to treatment with 10 nM of insulin for 10 min.

2.7. siRNA and plasmid transfections

For siRNA knockdown experiments, L6-G4-myc were transfected at 50% confluence with validated specific siRNA (Ctnnb1RSS331357; 5′-CCCAGAAUGCCGUUCGCCUUCAUUA-3′) or with control siRNA (Stealth™ RNAi siRNA Negative Control, Med GC). Transfections were performed in OptiMEM Reduced Serum Medium using Lipofectamine® 2000 and contained siRNA to a final concentration of 30 nM. For overexpression of β-catenin, L6-G4-myc or parental L6 cells were transfected with BcatWTdEGFP cDNA expression plasmid at 70% confluence using Lipofectamine® 2000 at a ratio of 1 ug DNA to 5 uL reagent. Prior to transfection, mutagenic primers were used to introduce the S552A amino acid change into the BcatWTdEGFP plasmid. Primer sequences were: 5′-AAGACATCACTGAGCCTGCC-3′ (forward) and 5′-GGCACGAGAGACTTGAGCTT-3′ (reverse). Mutagenesis PCR was performed using the GENEART® Site-Directed Mutagenesis Kit (ThermoFisher, Waltham, MA, USA) according to manufacturer's instructions, and the integrity of all vectors was

confirmed by sequencing of the β-catenin and GFP cDNA regions. All reagents for transfection experiments were from Life Technologies and used according to the manufacturer's instructions. BcatWT-dEGFP was a gift from Dr. Lucia Alonso-Gonzalez (University of Otago, Christchurch, New Zealand).

2.8. *In vitro* glucose uptake

For glucose uptake assays, differentiated L6-G4-myc were serum starved for 3 h in DMEM containing 0.2% BSA, then washed three times with sterile HEPES buffered saline (HBS; 140 mM NaCl, 20 μM HEPES, 2.5 mM MgSO4, 1 mM CaCl2, 5 mM KCl, pH 7.4, 25 °C). Cells were incubated for 10 min in HBS containing 100 mM 2-deoxyglucose and 0.1% BSA before a 20-minute pre-stimulation with insulin (10—100 nM). Cells were then incubated in HBS containing [3H]-2-deoxyglucose, 0.2% BSA and either vehicle controls or relevant treatment. After 10 min, glucose uptake was stopped by removing media and placing cells immediately on ice. Cells were lysed in 10% Triton X and read in for 1 min with a single label protocol. Glucose transport was expressed relative to respective protein concentrations, as determined by bicinchoninic acid (BCA) assay.

2.9. GLUT4 translocation assay

GLUT4 exocytosis was measured as previously described [26]. Briefly, L6-G4-myc and L6 myoblasts were cultured and transfected as described above. Following three hours of serum starvation, cells were stimulated with insulin (100 nM) for 10 min before being washed with ice-cold PBS, fixed with 3% paraformaldehyde for 10 min, blocked with 3% goat serum and incubated with polyclonal anti-Myc-Tag antibody (1:200) for 60 min at 4 °C. Following primary antibody incubation, cells were incubated with horseradish peroxidase (HRP)-conjugated goat anti-rabbit antibody (1:2,000) for 60 min at 4 °C. Cells were then washed with PBS and incubated with o-phenylenediamine dihydrochloride (OPD) for 20—30 min at room temperature. Incubation was stopped with 3 M of HCL and absorbance of the supernatant measured at 492 nM using a ThermoFisher Multiskan spectrophotometer (Thermofisher, Waltham, MA, USA). Background myc-tag binding was determined from L6 myoblasts that do not express the myc-tagged GLUT4 and subtracted from appropriate values.

2.10. Immunoblotting and polymerase chain reaction

Immunoblotting was performed as previously described [27]. For tissue, snap frozen muscle was minced using scissors in a lysis buffer containing Tris—HCl 20 mM, NaCl 150 mM, EDTA 1 mM, EGTA 1 mM, Triton X 1%, NP40 1%, NaPyro 2.5 mM, β-glycerol phosphate 1 mM, Na3VO4 1 mM and NaF 100 mM, then homogenised using a Qiagen tissuelyser. For cells, lysis buffer was added to plates before being scraped. In both cases, lysate was centrifuged at 4 °C at 20,000×*g* for 10 min. The resulting supernatant was resolved using sodium dodecyl sulphate-polyacrylamide gel electrophoresis (SDS-PAGE), following standard procedures. Membranes were incubated in primary antibody overnight at 4 °C (Supplementary Table 1) before being incubated in secondary antibody for 1—2 h at room temperature and imaged using chemiluminescence reagents. Fractionation was performed using the ThermoFisher subcellular fractionation kit for cultured cells (ThermoFisher, Waltham, MA, USA). Polymerase chain reaction (PCR) was performed as previously described [27]. RNA was extracted from frozen gastrocnemius muscle using Trizol reagent (Invitrogen, Carlsbad, CA) and a Direct-zol™ RNA MiniPrep (Zymo, Irvine, CA), and mRNA was reverse transcribed using the High-Capacity cDNA Reverse Transcription Kit (Applied Biosystems, Foster City, CA). Quantitative real-time PCR was performed on a ViiA™ 7 Real-Time PCR System (Applied Biosystems, Foster City, CA) using the SYBR Green Select Master Mix (Applied Biosystems, Foster City, CA). Reactions were performed in duplicate and relative quantification achieved using the ΔΔCt method with either 18S ribosomal RNA or hypoxanthine guanine phosphoribosyl transferase (HPRT) as an internal control. Primer sequences used are listed in Supplementary Table 2.

2.11. Assessment of actin dynamics

Actin dynamics were determined as previously described [28]. Briefly, L6-G4-myc cells were grown and differentiated into myotubes, stimulated with 100 nM of insulin and lysed in a actin stabilisation buffer (50 mM of PIPES, pH 6.9, 50 mM of NaCl, 5 mM of MgCl2, 5 mM of EGTA, 5% (v/v) glycerol, 0.1% Nonidet P-40, 0.1% Triton X-100, 0.1% Tween 20, 0.1% 2-mercaptoethanol, 0.001% Antifoam A, 1 mM of ATP, and protease inhibitors). Lysates were centrifuged for 5 min at 2,000×*g* at 37 °C, the supernatant was then recovered and centrifuged for 1 h at 100,000×*g* at 37 °C. The pellet (containing actin filamentous (F-actin)) was resuspended in Milli-Q water containing 10 μM of cytochalasin D, both the pellet fraction and the supernatant (G-actin containing) and were analysed by immunoblotting using anti-β-actin antibody alongside the G-actin-containing supernatant. Analysis was performed by summing the F and G fractions to give total actin and then expressing F-actin as a percentage of this total.

2.12. Immunoprecipitation and mass spectrometry

Immunoprecipitation was conducted as previously described [19]. L6-G4-myc cells were grown and differentiated before being stimulated with 100 nM of insulin. After 10 min, cells were lysed, and 1 mg of total protein was precleared with 50 μg of sepharose-A beads. Samples were incubated overnight with β-catenin-specific antibody, and the pulldown was performed using 50 μg of sepharose-A beads. Samples were washed once with lysis buffer and twice with water before being eluted with 5% acetic acid. Following elution, samples were dried by speed vac and resuspended in 50 μl of 50% ammonium bicarbonate, pH was adjusted to 7.8 and samples were reduced with 10 mM of dithiothreitol. Following reducing, samples were alkylated with 50 mM of iodoacetamide before being digested with 1 μg of analysis grade trypsin for 1 h at 45 °C. Samples were acidified with 5% formic acid and desalted via solid phase extraction. The analysis was performed on an Eksigent 425 nanoLC chromatography system (Sciex, Framingham MA, USA) connected to a TripleTOF 6600 mass spectrometer (Sciex, Framingham MA, USA). Samples were injected onto a 0.3 × 10 mm trap column packed with Reprosil C18 media and desalted for 5 min at 10 μl/min before being separated on a 0.075 × 200 mm PicoFrit column (New Objective) packed in-house with Reprosil C18 media. The following gradient was applied at 250 nl/min using a NanoLC 400 UPLC system (Eksigent): 0 min 5% B; 5 min 10%B; 22 min 15%B; 105 min 35%B; 110 min 98%B; 115 min 98%B; 116 min 5%B; 120 min 5%B, where A was 0.1% formic acid in water and B was 0.1% formic acid in acetonitrile.

The PicoFrit spray was directed into a TripleTOF 6600 quadrupole-time-of-flight mass spectrometer (Sciex, Framingham MA, USA) scanning from 350 to 1,600 *m/z* for 200 ms, followed by 40 ms MS/MS scans on the 50 most abundant multiply-charged peptides (100—1,600 *m/z*) for a total cycle time of 2.2 s. The mass spectrometer and high-performance liquid chromatography (HPLC) system were under the control of the Analyst TF 1.7 software package (Sciex, Framingham MA, USA). The resulting data were searched against a database comprising Uniprot rat and bovine entries appended with a set of common contaminant sequences (54,067 entries in total) using ProteinPilot version 5.0. Search parameters were as follows: Sample

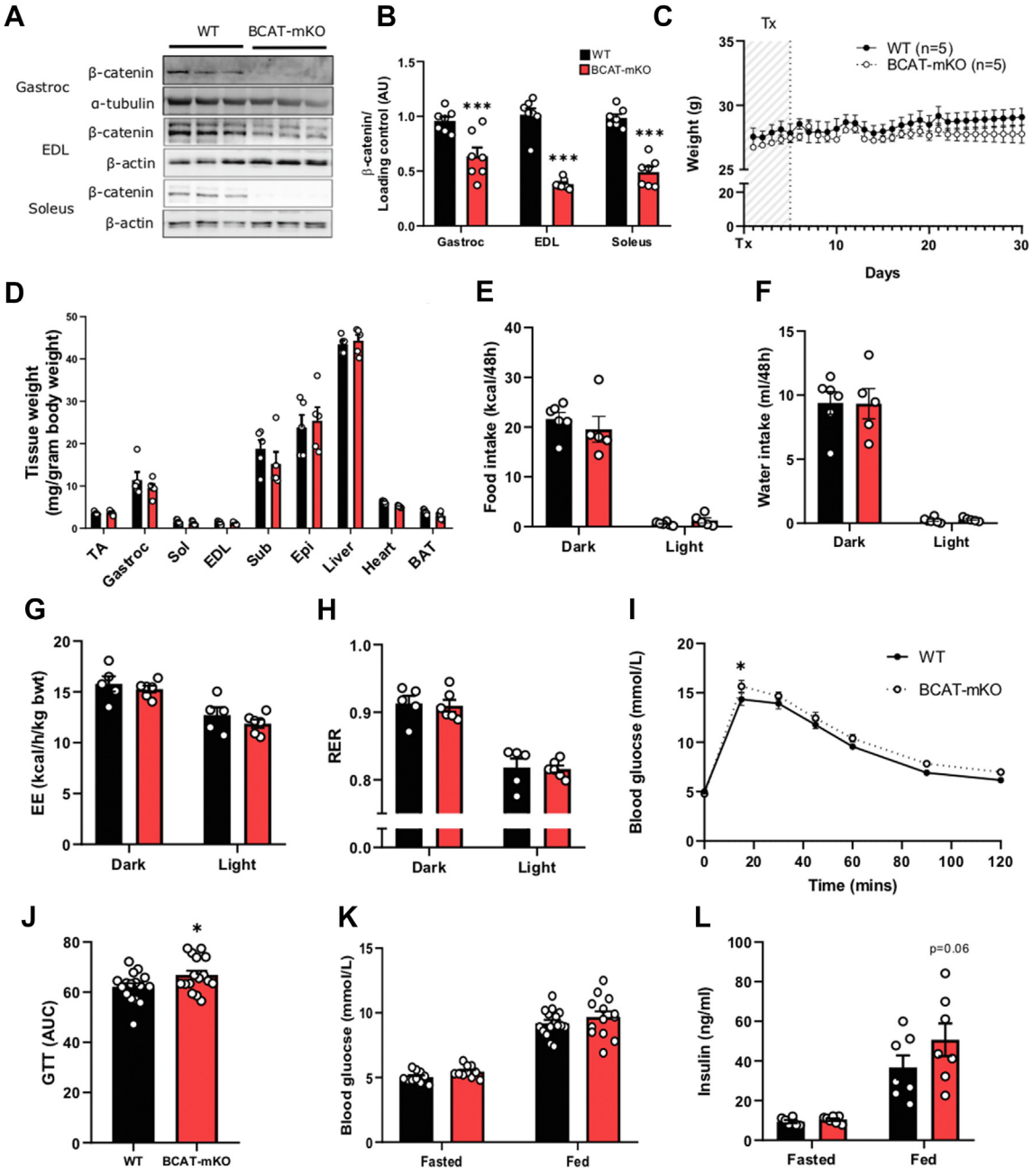

Figure 1: Depletion of β-catenin in skeletal muscle of adult mice mildly impairs glucose homeostasis without affecting tissue masses or energy expenditure. One month following tamoxifen (TX) treatment, β-catenin expression in gastrocnemius (gastroc), extensor digitorum longus (EDL), and soleus muscle (A–B), body mass (C), body composition (D), food and water intake (E–F), energy expenditure (G), respiratory exchange ratio (H), glucose tolerance (I–J), as well as fed and fasted blood glucose (K) and plasma insulin (L) were determined in WT and BCAT-mKO mice. Results are mean ± SE, with individual animals shown as data points in figures or in figure legend. Significance was determined using two-tailed Student's t-test (J), two-way ANOVA with LSD post-hoc analysis (B, D–H, K–L) or two-way RM ANOVA with LSD post-hoc analysis (C, I). TA, *tibialis anterior* muscle; sub, subcutaneous fat pad; epi, epididymal fat pad; BAT, brown adipose tissue. ***p $<$ 0.001 significance within groups.

Type, Identification; Search Effort, Thorough; Cys Alkylation, Yes; Digestion, Trypsin. The peptide summary exported from ProteinPilot was further processed in Excel using a custom macro to remove proteins with Unused Scores below 1.3, eliminate inferior or redundant peptide spectral matches and sum the intensities for all unique peptides from each protein. Contaminants were removed based on results from Uniprot and ProteinPilot, and label-free analysis was performed on the resulting peptide summary as previously described [29]. To be considered for further analysis, samples had at least two peptides identified with at least 95% confidence based on Protein Pilot analysis. Spectral intensity for each unique protein were standardised to the summed spectral intensity of each respective sample. Next, each resulting spectral intensity was expressed relative to the respective β-catenin intensities. To assess the effect of insulin, the ratio between each pair of PBS- or insulin-treated samples was then determined for every protein in that set of samples, and the ratio was recorded. A ratio >1 was considered an increase, while a ratio <1 was consider a decrease. Statistical significance was determined by a sign test [29].

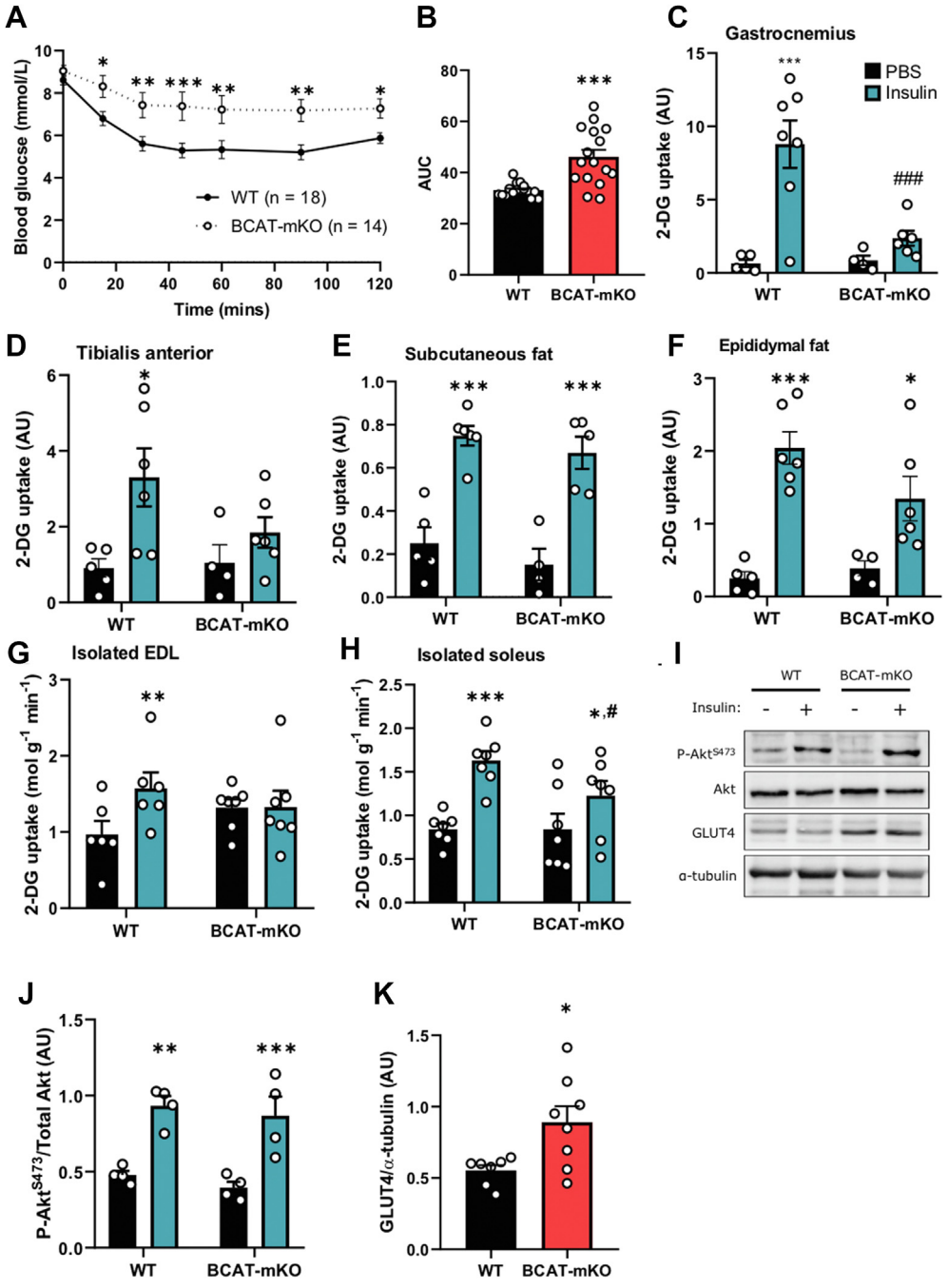

Figure 2: Reduced β-catenin in skeletal muscle of adult mice causes insulin resistance and impaired insulin-induced skeletal muscle glucose transport. One month following tamoxifen (TX) treatment, insulin tolerance was measured (A—B) before assessment of *in vivo* insulin-stimulated glucose transport into the gastrocnemius, tibialis anterior, subcutaneous and epididymal fat pads of BCAT-mKO and WT mice (C—F). Isolated muscle insulin-stimulated glucose transport was determined in EDL (extensor digitorium longus) and soleus muscle from WT and BCAT-mKO mice (G—H). Akt phosphorylation and GLUT4 protein expression in the gastrocnemius muscles of BCAT-mKO and WT mice was assessed by immunoblot (I—K). Results are mean ± SE, with individual animals shown as data points in figures or in figure legend. Significance was determined using two-tailed Student's t-test (B, K), two-way ANOVA with LSD post-hoc analysis (C—F, J) or two-way RM ANOVA with LSD post-hoc analysis (G—H). *$p < 0.05$, **$p < 0.01$, ***$p < 0.001$ significance within groups. #$p < 0.05$ significance between groups. AUC, area under curve.

2.13. Statistical analysis

All data are presented as mean ± SEM. Statistical significance was measured using 2-tailed Student's t-test and two-way analysis of variance (ANOVA) with Fisher's least significant difference (LSD) post-hoc analysis as indicated. The level of significance was set at $p < 0.05$ (GraphPad Prism version 8.0.0 for Windows, GraphPad Software, San Diego, CA, USA).

3. RESULTS

3.1. Depletion of skeletal muscle β-catenin expression in adult mice impairs glucose transport

To determine whether β-catenin is involved in the regulation of insulin-stimulated glucose transport, we generated inducible muscle-specific

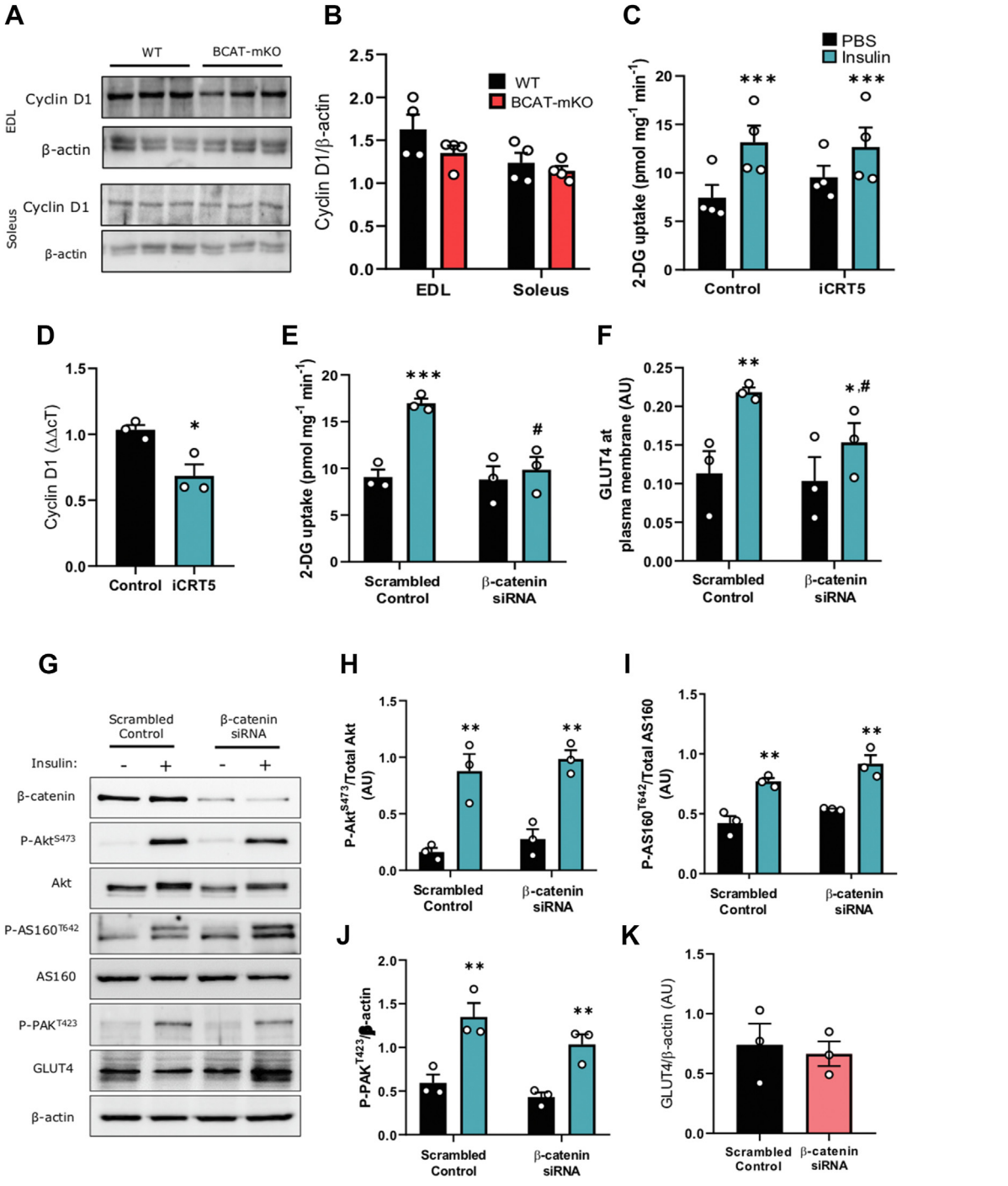

Figure 3: Depletion of β-catenin in L6-G4-myc cells impairs insulin-stimulated glucose transport and actin remodelling independent of Wnt-mediated transcription. Cyclin D1 protein expression in gastrocnemius muscle of BCAT-mKO and WT muscle was assessed by immunoblot (A—B). Glucose uptake and analysis of cyclin D1 mRNA expression in L6-G4-myc myoblasts treated with iCRT5 (50 μM) for 1 h (C—D). L6-G4-myc myoblasts were treated with β-catenin specific siRNA prior to assessment of glucose uptake (E—F) and insulin-signalling pathway (G—K). Results are mean ± SE, with individual animals or biological replicates shown as data points in figures or in figure legend. Significance was determined using two-tailed Student's t-test (D, K) or two-way ANOVA with LSD post-hoc analysis (B, C, E—J). *$p < 0.05$, ***$p < 0.001$ significance within groups. #$p < 0.05$ significance between groups.

β-catenin-deficient mice (BCAT-mKO). Four weeks following tamoxifen treatment of adult (8—12 week old) mice, β-catenin protein expression in gastrocnemius, extensor digitorum longus (EDL) and soleus muscles of BCAT-mKO mice were 40—60% lower than in control (WT) mice (Figure 1A—B), and β-catenin gene expression in gastrocnemius muscle of BCAT-mKO mice was 70% lower than WT mice (Supplementary Fig. 1a). Despite reduced skeletal muscle β-catenin expression, BCAT-mKO mice had similar β-catenin levels in non-skeletal muscle tissues (liver, heart, epididymal fat and subcutaneous fat; Supplementary Fig. 1b—c) and similar body and tissue masses

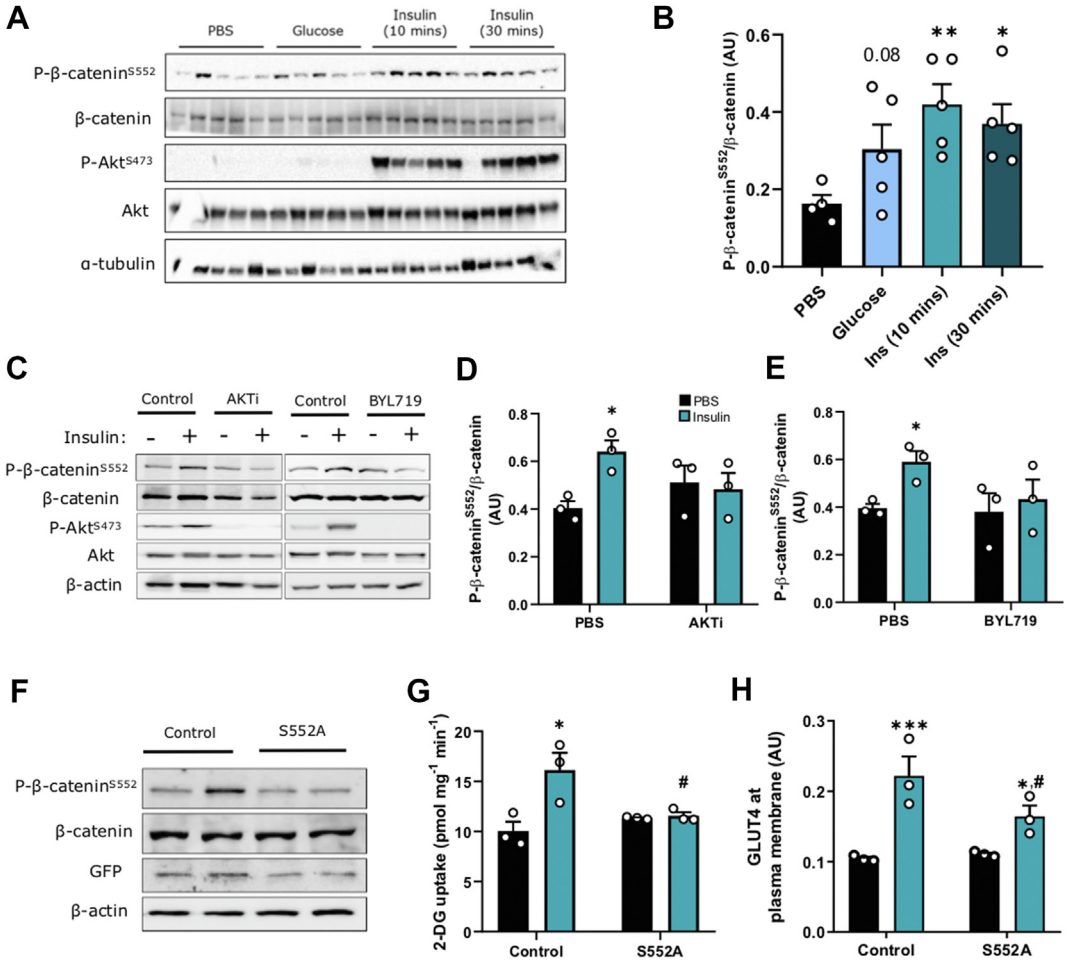

Figure 4: Insulin phosphorylates β-catenin^{S552} downstream of proximal insulin signalling, and β-catenin^{S552} phosphorylation is required for insulin-stimulated glucose transport. Immunoblotting analysis of P-β-catenin^{S552}, β-catenin, P-Akt^{S473} Akt, and β-actin in C57Bl/6j mice treated with either glucose or insulin prior to tissue collection (A—B). Immunoblotting analysis of P-β-catenin^{S552}, β-catenin, P-Akt^{S473}, Akt and β-actin in L6-G4-myc cells incubated with either BYL719 or AKTi-1/2 prior to insulin stimulation and (C—E). Insulin-stimulated glucose uptake and GLUT4 translocation to the membrane in L6-G4-myc cells transfected with S552A-β-catenin (F—H). Results are mean ± SE, with individual animals or biological replicates shown as individual data points in figures or in figure legend. Significance was determined using, one (B) or two-way ANOVA with LSD post-hoc analysis (D, E and G, H). *$p < 0.05$, **$p < 0.01$ significance within groups. #$p < 0.05$ significance between groups.

as WT mice (Figure 1C—D). BCAT-mKO mice food and water intake, energy expenditure and respiratory exchange ratio (RER) were similar to that of WT mice (Figure 1E—H). Consistent with the loss of β-catenin in skeletal muscle of adult mice not altering skeletal muscle mass, the ability of BCAT-mKO mice to perform treadmill exercise and voluntary physical activity levels were similar to that of WT mice (Supplementary Fig. 1d—g). To assess whether skeletal muscle-specific loss of β-catenin affects glucose homeostasis, we next performed an oral glucose tolerance test (GTT). Following a glucose bolus, BCAT-mKO had mildly elevated in blood glucose compared to WT (Figure 1I—J). Consistent with mildly impaired glucose homeostasis suggested by GTT, under fed conditions BCAT-mKO tended ($p = 0.06$) to have elevated plasma insulin levels for a similar blood glucose as WT mice (Figure 1K—L).

Despite only mild perturbations in glucose tolerance, BCAT-mKO mice had a substantially impaired ability to lower blood glucose following the intraperitoneal (i.p.) injection of an insulin bolus (Figure 2A—B, $p < 0.01$). To determine whether this might be associated with reduced skeletal muscle insulin sensitivity, we next measured *in vivo* glucose transport. Consistent with reduced insulin sensitivity, BCAT-mKO mice showed impaired uptake of glucose into gastrocnemius and tibialis anterior muscles following an i.p. glucose and insulin bolus (Figure 2C—D, $p < 0.01$); however, glucose uptake in subcutaneous and epididymal adipose tissue of BCAT-mKO mice was similar to that of WT (Figure 2E—F). To assess whether the reduced insulin-stimulated glucose transport is intrinsic to muscle, we measured glucose uptake in isolated EDL and soleus muscles from WT and BCAT-mKO mice. In response to insulin-stimulation, the ability of the EDL and soleus muscle to increase glucose transport was impaired in BCAT-mKO mice (Figure 2G—H). Reduced insulin-stimulated glucose transport in BCAT-mKO mice muscle did not appear to be the result of impaired canonical insulin signalling, as an i.p. bolus of insulin stimulated similar increases in Akt phosphorylation in the gastrocnemius muscles of WT and BCAT-mKO mice (Figure 2I—J). BCAT-mKO mice had increased expression of GLUT4 in the gastrocnemius (Figure 2K) and soleus muscles, but not EDL (Supplementary Fig. 1h).

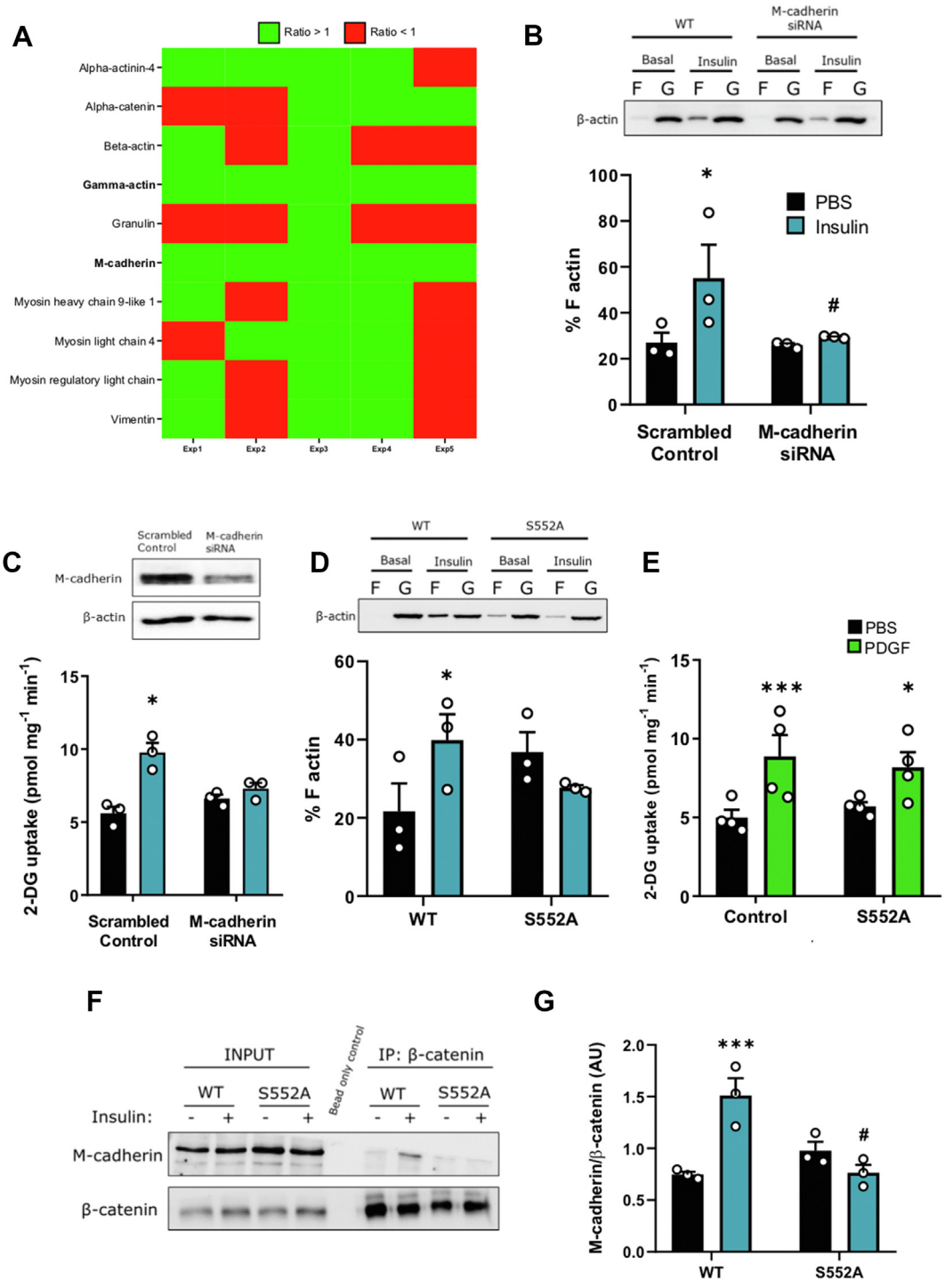

Figure 5: Insulin promotes β-catenin/M-cadherin interaction via β-catenin^{S552} phosphorylation. L6-G4-myc myotubes were treated with either insulin or PBS (control) prior to lysis and immunoprecipitation with β-catenin-specific antibody (A). L6-G4-myc myoblasts were treated with M-cadherin-specific siRNA prior to determination of F-actin % (B) and glucose uptake (C) following insulin stimulation. F actin % in response to insulin (D) and PDGF-mediated glucose uptake (E) and immunoblotting of M-cadherin following immunoprecipitation with anti-β-catenin antibody (F—G) in S552A-β-catenin expressing L6-G4-myc myoblasts. Results are mean ± SE, with biological replicates shown as individual data points in figures or in figure legend. Significance was determined using the sign-rank test (A) or two-way ANOVA with LSD post-hoc analysis (B—G). *$p < 0.05$, **$p < 0.01$, ***$p < 0.001$ significance within groups. #$p < 0.05$ significance between groups.

3.2. Phosphorylation of β-catenin^{S552} by proximal insulin signalling is critical for GLUT4 translocation and glucose uptake

Since β-catenin is canonically associated with the regulation of Wnt-related gene transcription, we next investigated whether impaired glucose transport in BCAT-mKO mice could be attributed to perturbed Wnt-signalling. Surprisingly, we found BCAT-mKO mice had similar skeletal muscle cyclin D1 protein expression WT (Figure 3A—B). Moreover, treatment of L6-G4-myc myotubes with the Wnt-selective

transcription inhibitor iCRT5, which selectively blocks β-catenin binding to Wnt transcription factors [30], did not affect insulin-stimulated glucose transport despite lowering cyclin D1 gene expression (Figure 3C—D). However, consistent with the BCAT-mKO mouse model, siRNA depletion of β-catenin in L6-G4-myc myoblasts attenuated insulin-stimulated glucose transport (Figure 3E—F) without affecting insulin-induced phosphorylation or expression of proximal insulin signalling intermediates Akt, AS160 or PAK^{T423}, which serves here as a surrogate marker for Rac1 activity (Figure 3G—K).

Because disruption of proximal insulin-signalling or Wnt-mediated transcription does not appear to explain the observed effect of β-catenin deletion on glucose uptake, we next investigated whether β-catenin is responsive to insulin signalling downstream of Akt. Following i.p. injection of insulin, β-catenin^{S552} phosphorylation in the gastrocnemius muscles from C57Bl/6j mice was increased after 10 and 30 min (Figure 4A—B), while there was a trend toward higher β-catenin^{S552} phosphorylation ($p = 0.08$) following i.p. injection of glucose. Consistent with this, β-catenin^{S552} phosphorylation was increased in L6-G4-myc myotubes following 10 min of insulin stimulation, and this effect was blocked with both the Akt inhibitor AKTi-1/2 and the p110α selective inhibitor of PI3k, BYL719 (Figure 4C—E), suggesting that the insulin-stimulated phosphorylation of β-catenin^{S552} is mediated by proximal insulin signalling. While inhibition of Rac1 with NSC23766 did not affect insulin-stimulated β-catenin^{S552} phosphorylation (Supplementary Fig. 2c—d), and β-catenin S675, Y142 and T654 phosphorylation were not affected by insulin stimulation of L6-G4-myc myotubes (Supplementary Fig. 2a—b). Next, we determined whether the phosphorylation of β-catenin^{S552} was required for insulin-stimulated glucose uptake by depleting endogenous β-catenin in L6-G4-myc myoblasts and then co-transfecting with either a plasmid carrying WT (control) β-catenin or a construct in which β-catenin serine 552 was mutated to an alanine (S552A), preventing its ability to be phosphorylated in response to insulin (Figure 4F). Similar to β-catenin siRNA-treated L6-G4-myc myoblasts, β-catenin S552A transfected L6-G4-myc myoblasts had reduced insulin-stimulated glucose uptake and GLUT4 translocation relative to controls (Figure 4G—H).

3.3. Insulin-stimulated β-catenin^{S552} promotes M-cadherin binding

Having uncovered a role for β-catenin in insulin-stimulated glucose uptake that is independent of transcription and proximal insulin signalling, we next set out to identify potential β-catenin insulin responsive binding partners using immunoprecipitation coupled with label-free mass spectrometry and proteomics. L6-G4-myc myotubes were treated with either PBS or insulin, then immunoprecipitated with anti-β-catenin antibody. The resulting immunoprecipitates were analysed for spectral intensity values of each identified protein and expressed relative to the corresponding β-catenin spectral intensity [29]. The ratios of each protein when in the insulin-stimulated and non-stimulated conditions were then determined (Figure 5A). Successful immunoprecipitation was confirmed by the presence of β-catenin's most well recognised binding partner, α-catenin, in all samples. Ten proteins were consistently detected across five independent experiments, of which two (M-cadherin and γ-actin) were significantly enriched in response to insulin (Figure 5A). M-cadherin, also known as cadherin-15, is a muscle-specific membrane bound cadherin protein, and γ-actin is an actin subunit, which is responsible for actin dynamics in muscle [31,32]. Given the role of actin cytoskeleton in *in vitro* glucose uptake, and the documented interactions between catenin and cadherin proteins, we chose to further investigate the interactions between β-catenin and M-cadherin in regulating insulin-stimulated glucose uptake and actin dynamics. β-catenin was confirmed to associated with M-cadherin in an insulin dependent manner via immunoblot (Supplementary Fig. 3a), and consistent with M-cadherin and β-catenin interacting at the cell membrane, insulin-stimulated β-catenin^{S552} phosphorylation was found to be membrane-specific (Supplementary Fig. 3b—c). Importantly, BCAT-mKO mice appear to express normal levels of M-cadherin relative to WT controls (Supplementary Fig. 3d—e).

Actin remodelling at the cell membrane is a key process in insulin-stimulated glucose uptake [6,20,33—35], and previous work has identified a role for β-catenin and cadherins in actin remodelling to facilitate insulin vesicle trafficking in pancreatic β-cells [28,36]. Therefore, we next assessed the role of M-cadherin in insulin-stimulated actin remodelling and glucose transport. Depletion of M-cadherin within L6-G4-myc cells attenuated insulin-induced actin polymerisation, as assessed by monitoring F-actin relative to total actin, and glucose transport (Figure 5B—C). Similarly, in S552A-β-catenin mutant cells, insulin did not induce F-actin formation, and these cells had greater levels of F-actin under basal conditions relative to WT controls (Figure 5D). To further test whether β-catenin^{S552} phosphorylation regulates glucose transport in an actin-dependent fashion, we investigated the effect of β-catenin^{S552} mutation on PDGF-BB-stimulated glucose uptake because PDGF-stimulated glucose uptake has been demonstrated to be resistant to actin disruption [6]. Unlike insulin stimulated glucose uptake, PDGF-BB was able to induce glucose uptake into L6-G4-myc myoblasts expressing S552A-β-catenin to a similar extent as in control cells (Figure 5E).

To assess whether the potential interactions between β-catenin, M-cadherin and actin regulation were β-catenin^{S552}-dependent, we next investigated β-catenin^{S552}-dependent insulin-mediated binding of β-catenin to M-cadherin via immunoblotting. Consistent with our hypothesis that insulin regulates β-catenin in muscle via β-catenin^{S552} phosphorylation, M-cadherin was present in β-catenin pulldowns from insulin-treated control but not S552A L6-G4-myc myotubes (Figure 5F—G). Together, these data support a model in which phosphorylation of β-catenin^{S552} by insulin promotes the binding of β-catenin to M-cadherin and that this interaction regulates insulin-stimulated glucose transport, potentially via regulating actin dynamics.

4. DISCUSSION

Insulin-stimulated skeletal muscle glucose uptake is important for maintaining whole body glucose homeostasis. While proximal signalling pathways that initiate GLUT4 translocation are reasonably well characterised [5,20,37—40], the downstream effectors which facilitate the physical changes in the actin cytoskeleton required to support GLUT4 movement to and fusion with the plasma membrane are less well defined [35,40—44]. Here, we report that the ablation of β-catenin in skeletal muscle impairs insulin sensitivity and insulin-stimulated skeletal muscle glucose uptake *in vivo*, in isolated muscle and in myocytes. Importantly, we provide evidence that the serine 552 phosphorylation site of β-catenin is involved in regulating insulin-induced GLUT4 membrane recruitment by interacting with muscle specific cell adhesion molecule M-cadherin to support insulin-mediated cortical actin remodelling. This is consistent with recent evidence that β-catenin is a regulator of GLUT4 trafficking in 3T3-L1 adipocytes [17] and acts as a signalling intermediate controlling vesicle movement across multiple tissues [28,45—47].

Our finding adds to the understanding of the processes regulating muscle insulin-stimulated glucose transport, and how insulin may regulate the reorganisation of the actin cytoskeleton to support GLUT4

trafficking to the cell membrane. Evidence to date has largely suggested that the Rac1/PAK1 signalling pathway controls many of the steps required for the insulin-mediated actin filament remodelling [5–7,35] required to aid GCV movement and membrane docking [6,48]; however, PAK1 may not be required for insulin-stimulated glucose transport *in vivo* [49]. Since β-catenin depletion impaired insulin-induced actin polymerisation independent of PAK phosphorylation, we propose that, in muscle, a second parallel pathway exists in which insulin signalling occurs via β-catenin to regulate actin remodelling at the cell membrane. In endothelial cells, E-cadherin provides a membrane-localised anchoring point for cortical F-actin synthesis to act upon, thereby pushing lateral membranes of cells together [50]. It is possible that, in muscle, M-cadherin could play a similar role in facilitating the formation of F-actin by providing structural support for new cortical actin filaments or the change in type of polymerisation occurring, i.e., from fibres to branches [4,51]. Importantly, β-catenin and M-cadherin were found to interact in a manner dependent on an insulin-induced phosphorylation of β-catenin^{S552}, and the knockdown of M-cadherin similarly impaired insulin-stimulated glucose transport and actin-polymerisation.

While insulin-regulated actin remodelling is well-established in cells, the role of actin reorganisation in the facilitation of glucose transport in mature muscle is less clear. Indeed, recently it has been reported that germline muscle-specific β-actin knockout (KO) has limited impact on isolated muscle glucose transport [52]. Since actin plays an important role in muscle [53], it is possible that germline knockout of β-actin leads to compensatory adaptations to overcome the need of actin reorganisation for optimal *ex vivo* glucose transport. Indeed, skeletal muscle β-catenin is also essential for development, with germline muscle-specific knockout being lethal at a young age [54]. However, in our model, in which β-catenin ablation was induced in adult mice, the loss of β-catenin did not affect muscle size or function (as determined by exercise performance), suggesting a differential role for β-catenin in growth and development. Furthermore, β-actin is only one of several actin isoforms found in muscle, which include α and γ-actin, the latter of which was identified here as associating with β-catenin following insulin stimulation, and is considered to play a more regulatory role in actin dynamics [53]. The specific signalling pathways and events which regulate β-catenin's role in actin cytoskeleton remodelling are not fully elucidated, and it is possible that β-catenin integrates with the established actin-cytoskeleton regulating pathways via interactions with Rac1 [7]. While our data suggest that β-catenin is downstream of Akt in the insulin signalling cascade, and Rac1 has been suggested to be involved in insulin-stimulated actin cytoskeleton reorganisation independent of Akt [7], this conflicts with reports that Rac1 may also be downstream of Akt [8]. Whether and how these pathways work together to regulate actin reorganisation during GLUT4 trafficking and therefore how β-catenin fits into the system requires further attention.

Early-stage insulin resistance is often characterised by dysfunctional glucose transport despite normal proximal insulin signalling [55–57]. This suggests that the initial dysfunction in insulin-stimulated glucose transport is downstream or independent of PI3k/Akt signalling. Our data suggests that β-catenin^{S552} functions downstream of PI3k/Akt mediated signalling and that loss of β-catenin impairs insulin-stimulated glucose transport independent of Akt/AS160. Therefore, β-catenin is a possible site of dysfunction in early stage insulin resistance via its role in actin remodelling. Previous work investigating insulin-mediated actin remodelling during the onset of insulin-resistance is limited. However, it is clear in both *in vitro* and *in vivo* models that actin remodelling is impaired during insulin-resistance, with both palmitate and high-insulin-/high glucose-treated myotubes as well as high-fat diet fed mice displaying impaired actin cytoskeleton remodelling [48,58]. Determining whether this is due to dysfunction of downstream actin regulating proteins such as β-catenin or through impaired upstream signalling should be considered in further research.

Typically, phosphorylation of β-catenin^{S552} is associated with increased transcription and nuclear accumulation [13,59–61], meaning that transcriptionally mediated effects of β-catenin suppression could also be affecting insulin-stimulated glucose transport and GLUT4 trafficking. Indeed, previous work found that hepatic β-catenin^{S552} is phosphorylated by glucagon and that this increased transcription of cyclin D1 and c-Myc [62]. However, our data that β-catenin ablation in muscle did not affect Wnt-signalling-related gene expression and that selectively blocking β-catenin binding to Wnt transcription factors did not affect insulin-stimulated glucose transport suggests that insulin-mediated β-catenin^{S552} phosphorylation plays a non-transcriptional role regulating glucose transport. Consistent with this, the majority of phosphorylated β-catenin^{S552} appears at the membrane following insulin stimulation (rather than the nucleus), and β-catenin^{S552} has been shown to readily associate with cadherin proteins at the membrane in colorectal adenocarcinoma cells [63]. One potential explanation for these contrasting observations is that there are distinct cellular pools of β-catenin [64], and although phosphorylation of nuclear associated β-catenin^{S552} may promote gene expression through transcription factor binding, phosphorylation of serine 552 of cell–cell adhesion-associated β-catenin could specifically promote binding to cadherin proteins. However, nuclear and cell membrane localisation of β-catenin may not be mutually exclusive since the association of β-catenin with different binding partners is dependent on the affinity of the binding partners at overlapping binding sites in the central region of β-catenin. Transcription co-factors and cadherins have similar binding affinities to these regions of β-catenin [65], and therefore relative expression of different binding partners is likely to be a major driver of β-catenin localisation. Phosphorylation of β-catenin can also change binding partner preferences [65], and in muscle, it is possible that insulin-induced β-catenin^{S552} enhances binding affinity of β-catenin to adhesion partners over transcription factors.

Taken together, our data indicate that β-catenin is involved in transcription-independent insulin-mediated remodelling of the actin cytoskeleton in skeletal muscle to support GLUT4 membrane trafficking and glucose uptake. Furthermore, we provide evidence that M-cadherin is a novel regulator of insulin-mediated glucose transport in skeletal muscle and link β-catenin^{S552} phosphorylation to insulin-stimulated M-cadherin binding and actin reorganisation. This supports a role for β-catenin in regulating glucose homeostasis, and future studies should address whether dysfunctional β-catenin-regulated cytoskeleton dynamics are involved in the development of skeletal muscle insulin resistance and whether β-catenin is required for other modes of glucose transport.

AUTHOR CONTRIBUTIONS

Author contributions: SWCM, BS, PRS and TLM designed the research; SWCM and TLM performed the research; SWCM, BS, PRS and TLM analysed the data; and SWCM, PRS and TLM wrote the paper.

ACKNOWLEDGEMENTS

This study was funded by the Rutherford Discovery Fellowship and the University of Auckland Faculty Research Development Fund (all to TLM) and the Maurice Wilkins Centre for Molecular Biodiscovery (SWCM). We would like to thank Martin

Middleditch and Bincy Jacobs from the Auckland University Mass Spectrometry hub (MaSH) and Fengyun (Fiona) Hu and Waruni Dissanayake for their technical assistance. Graphical abstract was created with BioRender.com.

CONFLICT OF INTEREST

None declared.

APPENDIX A. SUPPLEMENTARY DATA

Supplementary data to this article can be found online at https://doi.org/10.1016/j.molmet.2020.101091.

REFERENCES

[1] DeFronzo, R.A., Ferrannini, E., 1987. Regulation of hepatic glucose metabolism in humans. Diabetes/Metabolism Research and Reviews 3(2):415–459.

[2] Mîinea, C.P., Sano, H., Kane, S., Sano, E., Fukuda, M., Peränen, J., et al., 2005. AS160, the Akt substrate regulating GLUT4 translocation, has a functional Rab GTPase-activating protein domain. Biochemical Journal 391(1):87–93.

[3] Wang, Q., Somwar, R., Bilan, P.J., Liu, Z., Jin, J., Woodgett, J.R., et al., 1999. Protein kinase B/Akt participates in GLUT4 translocation by insulin in L6 myoblasts. Molecular and Cellular Biology 19(6):4008–4018.

[4] Tunduguru, R., Zhang, J., Aslamy, A., Salunkhe, V.A., Brozinick, J.T., Elmendorf, J.S., et al., 2017. The actin-related p41ARC subunit contributes to p21-activated kinase-1 (PAK1)-mediated glucose uptake into skeletal muscle cells. Journal of Biological Chemistry, 801340. M117.

[5] Tunduguru, R., Chiu, T.T., Ramalingam, L., Elmendorf, J.S., Klip, A., Thurmond, D.C., 2014. Signaling of the p21-activated kinase (PAK1) coordinates insulin-stimulated actin remodeling and glucose uptake in skeletal muscle cells. Biochemical Pharmacology 92(2):380–388.

[6] Török, D., Patel, N., JeBailey, L., Thong, F.S., Randhawa, V.K., Klip, A., et al., 2004. Insulin but not PDGF relies on actin remodeling and on VAMP2 for GLUT4 translocation in myoblasts. Journal of Cell Science 117(22):5447–5455.

[7] Sylow, L., Kleinert, M., Pehmøller, C., Prats, C., Chiu, T.T., Klip, A., et al., 2014. Akt and Rac1 signaling are jointly required for insulin-stimulated glucose uptake in skeletal muscle and downregulated in insulin resistance. Cellular Signalling 26(2):323–331.

[8] Takenaka, N., Araki, N., Satoh, T., 2019. Involvement of the protein kinase Akt2 in insulin-stimulated Rac1 activation leading to glucose uptake in mouse skeletal muscle. PloS One 14(2):e0212219.

[9] Sylow, L., Jensen, T.E., Kleinert, M., Mouatt, J.R., Maarbjerg, S.J., Jeppesen, J., et al., 2013. Rac1 is a novel regulator of contraction-stimulated glucose uptake in skeletal muscle. Diabetes 62(4):1139–1151.

[10] Møller, L.L., Jaurji, M., Kjøbsted, R., Joseph, G.A., Madsen, A.B., Knudsen, J.R., et al., 2019. Insulin-stimulated glucose uptake partly relies on p21-activated kinase (PAK)-2, but not PAK1, in Mouse skeletal muscle. bioRxiv, 543736.

[11] Maschio, D.A., Oliveira, R.B., Santos, M.R., Carvalho, C.P.F., Barbosa-Sampaio, H.C.L., Collares-Buzato, C.B., 2016. Activation of the Wnt/beta-catenin pathway in pancreatic beta cells during the compensatory islet hyperplasia in prediabetic mice. Biochemical and Biophysical Research Communications 478(4):1534–1540.

[12] Clevers, H., Nusse, R., 2012. Wnt/β-catenin signaling and disease. Cell 149(6):1192–1205.

[13] Valenta, T., Hausmann, G., Basler, K., 2012. The many faces and functions of β-catenin. The EMBO Journal 31(12):2714–2736.

[14] Venerando, A., Girardi, C., Ruzzene, M., Pinna, L.A., 2013. Pyrvinium pamoate does not activate protein kinase CK1, but promotes Akt/PKB down-regulation and GSK3 activation. Biochemical Journal 452(1):131–137.

[15] Liu, C., Li, Y., Semenov, M., Han, C., Baeg, G.-H., Tan, Y., et al., 2002. Control of β-catenin phosphorylation/degradation by a dual-kinase mechanism. Cell 108(6):837–847.

[16] Chaudhuri, R., Khoo, P.S., Tonks, K., Junutula, J.R., Kolumam, G., Modrusan, Z., et al., 2015. Cross-species gene expression analysis identifies a novel set of genes implicated in human insulin sensitivity. NPJ Systems Biology and Applications 1:15010.

[17] Dissanayake, W.C., Sorrenson, B., Cognard, E., Hughes, W.E., Shepherd, P.R., 2018. β-catenin is important for the development of an insulin responsive pool of GLUT4 glucose transporters in 3T3-L1 adipocytes. Experimental Cell Research.

[18] Zhu, G., Wang, Y., Huang, B., Liang, J., Ding, Y., Xu, A., et al., 2012. A Rac1/PAK1 cascade controls β-catenin activation in colon cancer cells. Oncogene 31(8):1001.

[19] Tian, Q., Feetham, M.C., Tao, W.A., He, X.C., Li, L., Aebersold, R., et al., 2004. Proteomic analysis identifies that 14-3-3ζ interacts with β-catenin and facilitates its activation by Akt. Proceedings of the National Academy of Sciences 101(43):15370–15375.

[20] Lim, C.-Y., Bi, X., Wu, D., Kim, J.B., Gunning, P.W., Hong, W., et al., 2015. Tropomodulin3 is a novel Akt2 effector regulating insulin-stimulated GLUT4 exocytosis through cortical actin remodeling. Nature Communications 6:5951.

[21] Brault, V., Moore, R., Kutsch, S., Ishibashi, M., Rowitch, D.H., McMahon, A.P., et al., 2001. Inactivation of the (β)-catenin gene by Wnt1-Cre-mediated deletion results in dramatic brain malformation and failure of craniofacial development. Development 128(8):1253–1264.

[22] McCarthy, J.J., Srikuea, R., Kirby, T.J., Peterson, C.A., Esser, K.A., 2012. Inducible Cre transgenic mouse strain for skeletal muscle-specific gene targeting. Skeletal Muscle 2(1):8.

[23] Lundell, L.S., Massart, J., Altıntaş, A., Krook, A., Zierath, J.R., 2019. Regulation of glucose uptake and inflammation markers by FOXO1 and FOXO3 in skeletal muscle. Molecular Metabolism 20:79–88.

[24] Campbell, S., Febbraio, M., 2002. Effect of the ovarian hormones on GLUT4 expression and contraction-stimulated glucose uptake. American Journal of Physiology - Endocrinology And Metabolism 282(5):E1139–E1146.

[25] Merry, T.L., Steinberg, G.R., Lynch, G.S., McConell, G.K., 2009. Skeletal muscle glucose uptake during contraction is regulated by nitric oxide and ROS independently of AMPK. American Journal of Physiology - Heart and Circulatory Physiology.

[26] Wang, Q., Khayat, Z., Kishi, K., Ebina, Y., Klip, A., 1998. GLUT4 translocation by insulin in intact muscle cells: detection by a fast and quantitative assay. FEBS Letters 427(2):193–197.

[27] Merry, T.L., Brooks, A.E., Masson, S.W., Adams, S.E., Jaiswal, J.K., Jamieson, S.M., et al., 2020. The CSF1 receptor inhibitor pexidartinib (PLX3397) reduces tissue macrophage levels without affecting glucose homeostasis in mice. International Journal of Obesity 44(1):245–253.

[28] Sorrenson, B., Cognard, E., Lee, K.L., Dissanayake, W.C., Fu, Y., Han, W., et al., 2016. A critical role for β-catenin in modulating levels of insulin secretion from β-cells by regulating actin cytoskeleton and insulin vesicle localization. Journal of Biological Chemistry 291(50):25888–25900.

[29] Geetha, T., Langlais, P., Luo, M., Mapes, R., Lefort, N., Chen, S.-C., et al., 2011. Label-free proteomic identification of endogenous, insulin-stimulated interaction partners of insulin receptor substrate-1. Journal of the American Society for Mass Spectrometry 22(3):457–466.

[30] Gonsalves, F.C., Klein, K., Carson, B.B., Katz, S., Ekas, L.A., Evans, S., et al., 2011. An RNAi-based chemical genetic screen identifies three small-molecule inhibitors of the Wnt/wingless signaling pathway. Proceedings of the National Academy of Sciences 108(15):5954–5963.

[31] Donalies, M., Cramer, M., Ringwald, M., Starzinski-Powitz, A., 1991. Expression of M-cadherin, a member of the cadherin multigene family, correlates with differentiation of skeletal muscle cells. Proceedings of the National Academy of Sciences 88(18):8024–8028.

[32] Belyantseva, I.A., Perrin, B.J., Sonnemann, K.J., Zhu, M., Stepanyan, R., McGee, J., et al., 2009. γ-Actin is required for cytoskeletal maintenance but not development. Proceedings of the National Academy of Sciences 106(24): 9703–9708.

[33] Kee, A.J., Yang, L., Lucas, C.A., Greenberg, M.J., Martel, N., Leong, G.M., et al., 2015. An actin filament population defined by the tropomyosin Tpm3. 1 regulates glucose uptake. Traffic 16(7):691–711.

[34] Nazari, H., Khaleghian, A., Takahashi, A., Harada, N., Webster, N., Nakano, M., et al., 2011. Cortactin, an actin binding protein, regulates GLUT4 translocation via actin filament remodeling. Biochemistry (Moscow) 76(11):1262–1269.

[35] Chiu, T.T., Patel, N., Shaw, A.E., Bamburg, J.R., Klip, A., 2010. Arp2/3-and cofilin-coordinated actin dynamics is required for insulin-mediated GLUT4 translocation to the surface of muscle cells. Molecular Biology of the Cell 21(20):3529–3539.

[36] Dissanayake, W.C., Sorrenson, B., Lee, K.L., Barre, S., Shepherd, P.R., 2020. α-catenin isoforms are regulated by glucose and involved in regulating insulin secretion in rat clonal β-cell models. Biochemical Journal 477(4):763–772.

[37] Tunduguru, R., Zhang, J., Aslamy, A., Salunkhe, V.A., Brozinick, J.T., Elmendorf, J.S., et al., 2017. The actin-related p41ARC subunit contributes to p21-activated kinase-1 (PAK1)–mediated glucose uptake into skeletal muscle cells. Journal of Biological Chemistry 292(46):19034–19043.

[38] Lombardo, A.T., Kennedy, G.G., Nelson, S.R., Trybus, K.M., Warshaw, D.M., 2017. Myova vesicle transport through biomimetic actin networks visualized by 3D storm microscopy. Biophysical Journal 112(3):272a–273a.

[39] Sun, Y., Jaldin-Fincati, J., Liu, Z., Bilan, P.J., Klip, A., 2016. A complex of Rab13 with MICAL-L2 and α-actinin-4 is essential for insulin-dependent GLUT4 exocytosis. Molecular Biology of the Cell 27(1):75–89.

[40] Klip, A., McGraw, T.E., James, D.E., 2019. 30 sweet years of GLUT4. Journal of Biological Chemistry 008351. REV119.

[41] Tanaka, K., Takeda, S., Mitsuoka, K., Oda, T., Kimura-Sakiyama, C., Maéda, Y., et al., 2018. Structural basis for cofilin binding and actin filament disassembly. Nature Communications 9(1):1–12.

[42] Bamburg, J.R., Bernstein, B.W., 2010. Roles of ADF/cofilin in actin polymerization and beyond. F1000 Biology Reports 2.

[43] Nishita, M., Wang, Y., Tomizawa, C., Suzuki, A., Niwa, R., Uemura, T., et al., 2004. Phosphoinositide 3-kinase-mediated activation of cofilin phosphatase Slingshot and its role for insulin-induced membrane protrusion. Journal of Biological Chemistry 279(8):7193–7198.

[44] Gohla, A., Bokoch, G.M., 2002. 14-3-3 regulates actin dynamics by stabilizing phosphorylated cofilin. Current Biology 12(19):1704–1710.

[45] Sun, Y., Aiga, M., Yoshida, E., Humbert, P.O., Bamji, S.X., 2009. Scribble interacts with β-catenin to localize synaptic vesicles to synapses. Molecular Biology of the Cell 20(14):3390–3400.

[46] Su, Z., Deshpande, V., James, D.E., Stöckli, J., 2018. Tankyrase modulates insulin sensitivity in skeletal muscle cells by regulating the stability of GLUT4 vesicle proteins. Journal of Biological Chemistry 293(22):8578–8587.

[47] Bamji, S.X., Shimazu, K., Kimes, N., Huelsken, J., Birchmeier, W., Lu, B., et al., 2003. Role of β-catenin in synaptic vesicle localization and presynaptic assembly. Neuron 40(4):719–731.

[48] Tong, P., Khayat, Z.A., Huang, C., Patel, N., Ueyama, A., Klip, A., 2001. Insulin-induced cortical actin remodeling promotes GLUT4 insertion at muscle cell membrane ruffles. Journal of Clinical Investigation 108(3):371–381.

[49] Møller, L.L.V., Jaurji, M., Kjøbsted, R., Joseph, G.A., Madsen, A.B., Knudsen, J.R., et al., 2020. Insulin-stimulated glucose uptake partly relies on p21-activated kinase 2 (PAK2), but not PAK1, in mouse skeletal muscle. The Journal of Physiology.

[50] Li, J.X.H., Tang, V.W., Brieher, W.M., 2020. Actin protrusions push at apical junctions to maintain E-cadherin adhesion. Proceedings of the National Academy of Sciences 117(1):432–438.

[51] Brozinick, J.T., Berkemeier, B.A., Elmendorf, J.S., 2007. "Actin" g on GLUT4: membrane & cytoskeletal components of insulin action. Current Diabetes Reviews 3(2):111–122.

[52] Madsen, A.B., Knudsen, J.R., Henriquez-Olguin, C., Angin, Y., Zaal, K.J., Sylow, L., et al., 2018. β-Actin shows limited mobility and is required only for supraphysiological insulin-stimulated glucose transport in young adult soleus muscle. American Journal of Physiology - Endocrinology And Metabolism 315(1):E110–E125.

[53] Dugina, V., Shagieva, G., Kopnin, P., 2019. Biological role of actin isoforms in mammalian cells. Biochemistry (Moscow) 84(6):583–592.

[54] Paris, N.D., Coles, G.L., Ackerman, K.G., 2015. Wt1 and β-catenin cooperatively regulate diaphragm development in the mouse. Developmental Biology 407(1):40–56.

[55] Karlsson, H.K., Zierath, J.R., Kane, S., Krook, A., Lienhard, G.E., Wallberg-Henriksson, H., 2005. Insulin-stimulated phosphorylation of the Akt substrate AS160 is impaired in skeletal muscle of type 2 diabetic subjects. Diabetes 54(6):1692–1697.

[56] Kim, Y.-B., Nikoulina, S.E., Ciaraldi, T.P., Henry, R.R., Kahn, B.B., 1999. Normal insulin-dependent activation of Akt/protein kinase B, with diminished activation of phosphoinositide 3-kinase, in muscle in type 2 diabetes. Journal of Clinical Investigation 104(6):733–741.

[57] Krook, A., Roth, R.A., Jiang, X.J., Zierath, J.R., Wallberg-Henriksson, H., 1998. Insulin-stimulated Akt kinase activity is reduced in skeletal muscle from NIDDM subjects. Diabetes 47(8):1281–1286.

[58] Brozinick, J.T., Hawkins, E.D., Strawbridge, A.B., Elmendorf, J.S., 2004. Disruption of cortical actin in skeletal muscle demonstrates an essential role of the cytoskeleton in glucose transporter 4 translocation in insulin-sensitive tissues. Journal of Biological Chemistry 279(39):40699–40706.

[59] Zhang, J., Shemezis, J.R., McQuinn, E.R., Wang, J., Sverdlov, M., Chenn, A., 2013. AKT activation by N-cadherin regulates beta-catenin signaling and neuronal differentiation during cortical development. Neural Development 8(1):7.

[60] Zhao, J., Yue, W., Zhu, M.J., Sreejayan, N., Du, M., 2010. AMP-activated protein kinase (AMPK) cross-talks with canonical Wnt signaling via phosphorylation of β-catenin at Ser 552. Biochemical and Biophysical Research Communications 395(1):146–151.

[61] Cognard, E., Dargaville, C.G., Hay, D.L., Shepherd, P.R., 2013. Identification of a pathway by which glucose regulates beta-catenin signalling via the cAMP/protein kinase A pathway in beta-cell models. Biochemical Journal 449(3): 803–811.

[62] Chowdhury, M.K.H., Montgomery, M.K., Morris, M.J., Cognard, E., Shepherd, P.R., Smith, G.C., 2015. Glucagon phosphorylates serine 552 of beta-catenin leading to increased expression of cyclin D1 and c-Myc in the isolated rat liver. Archives of Physiology and Biochemistry 121(3):88–96.

[63] Maher, M.T., Mo, R., Flozak, A.S., Peled, O.N., Gottardi, C.J., 2010. β-Catenin phosphorylated at serine 45 is spatially uncoupled from β-catenin phosphorylated in the GSK3 domain: implications for signaling. PloS One 5(4): e10184.

[64] Gottardi, C.J., Gumbiner, B.M., 2004. Distinct molecular forms of β-catenin are targeted to adhesive or transcriptional complexes. The Journal of Cell Biology 167(2):339–349.

[65] Choi, H.J., Huber, A.H., Weis, W.I., 2006. Thermodynamics of beta-catenin-ligand interactions: the roles of the N- and C-terminal tails in modulating binding affinity. Journal of Biological Chemistry 281(2):1027–1038.

